Outflow boundaries

What is it?
- Relatively cool gust of wind produced by showers and thunderstorms
- Air hits ground from storm downdraft and spreads outward
- Depth of 100s of m to several km.
- Rapid drop in local θ_e

Basic conceptual physics
- Rain falls into subsaturated air and evaporates, below cloud base
- Because rain cooled air is colder and denser it sinks, helping to form a local area of high pressure at surface (mesohigh)
- Additional entrainment of dry air into updraft above cloud base can also cause evaporation, melting, sublimation of hydrometeors. May also contribute to strength of downdraft.

Gust front: leading edge of outflow boundary. Can be potential initiation point for new cells. Detect by 1) radar signatures and) VIS satellite imagery

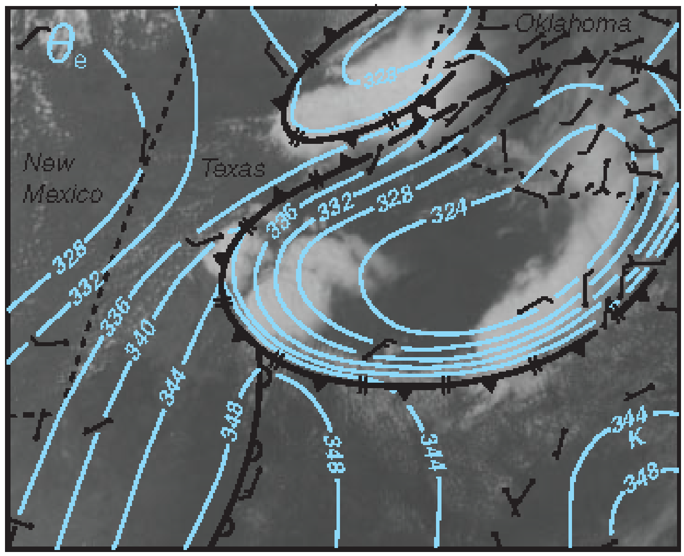

Figure 5.20 Visible satellite image of convective outflow from 2000 UTC 31 May 1995, with θ_e contours overlaid. Outflow boundaries are indicated using the symbology introduced in Figure 5.1. A dryline (Section 5.2) is also analyzed using unfilled scallops. (Adapted from Wakimoto *et al.* [2004b].)

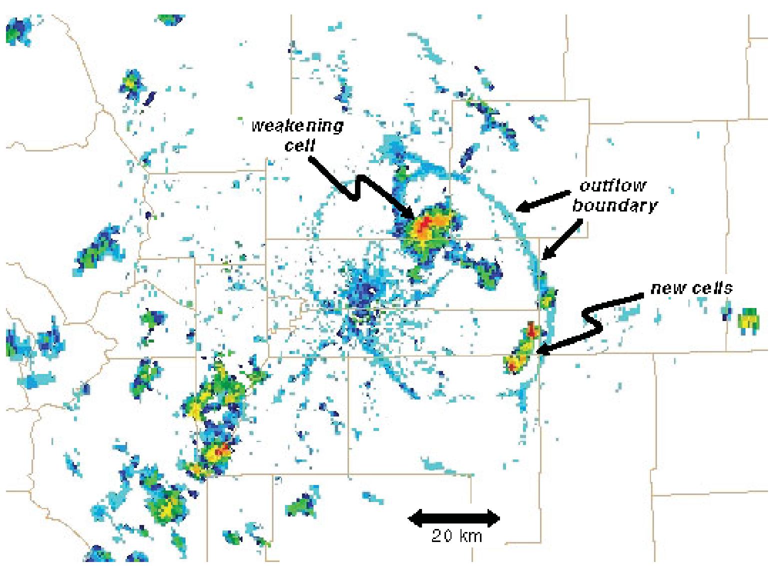

Figure 5.21 Radar reflectivity image showing a nearly circular outflow boundary produced by storms east of Denver, CO, manifested as a reflectivity fine-line.

Figure 5.22 Photograph of a shelf cloud along the leading edge of an outflow boundary. Photograph by Eric Nguyen.

Bucks County, Pennsylvania (Washington Post)

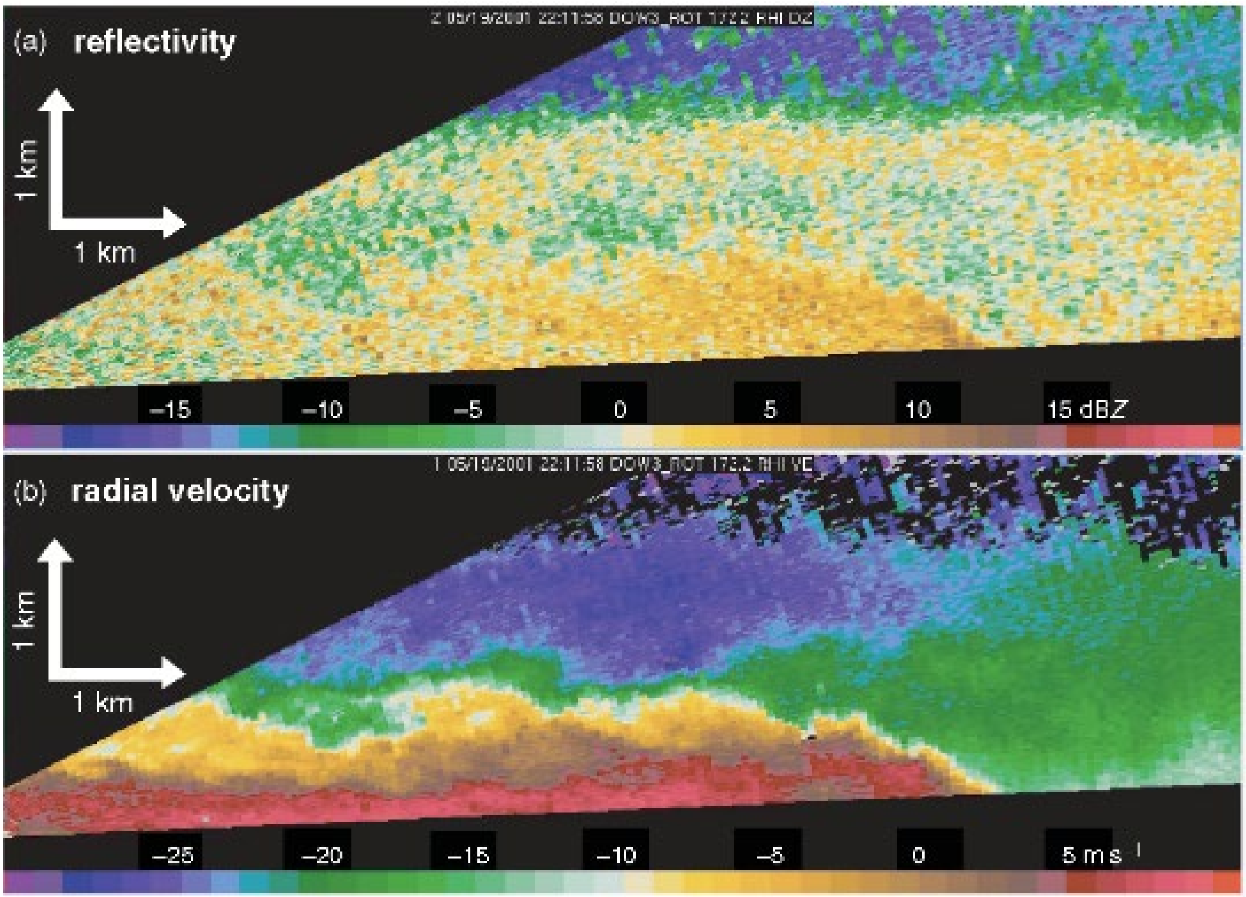

Figure 5.26 Radar observations of a gust front (moving from left to right) having density current characteristics. The data were obtained by the Doppler On Wheels (DOW) radar. (a) Reflectivity factor (reflectivities are uncalibrated) in dBZ. (b) Radial velocity in m s^{-1}.

Strength of outflow function of
- environmental profiles of T, RH
- cloud base, depth of PBL
- microphysical characteristics of the specific storm.

=) Coldest outflows tend to be produced by high-based thunderstorms, that rain into very dry PBLs. Very typical of southwest US!!

Mesohighs, mesolows

Mesohighs: A local increase in atmospheric pressure following passage of gust front
- Hydrostatic effects: increase in mass of air
- Dynamic effects: where air is being deflected and/or decelerated.

Mesolows: In larger, more organized convective systems (eg. squall lines, MCSs) a region of low pressure develops following the outflow. Occurs due to unsaturated decent, subsidence, warming at mid-levels, after passage of a leading convective line.

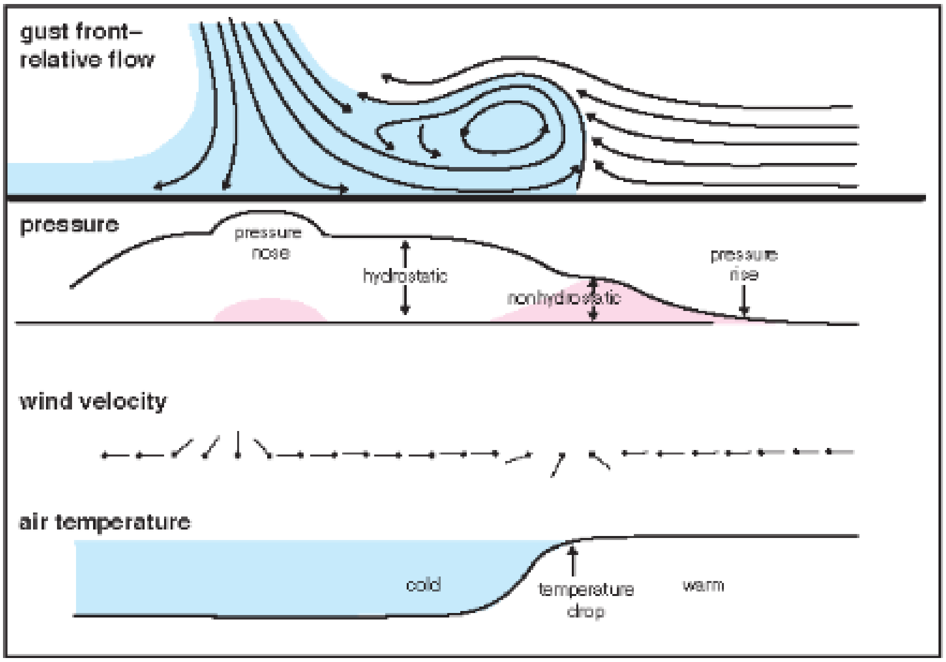

Figure 5.23 Conceptual model of surface observations during the passage of a gust front in its mature stage. Note that part of the pressure excess is due to nonhydrostatic effects (cf. Figure 2.6). (Adapted from Wakimoto [1982].)

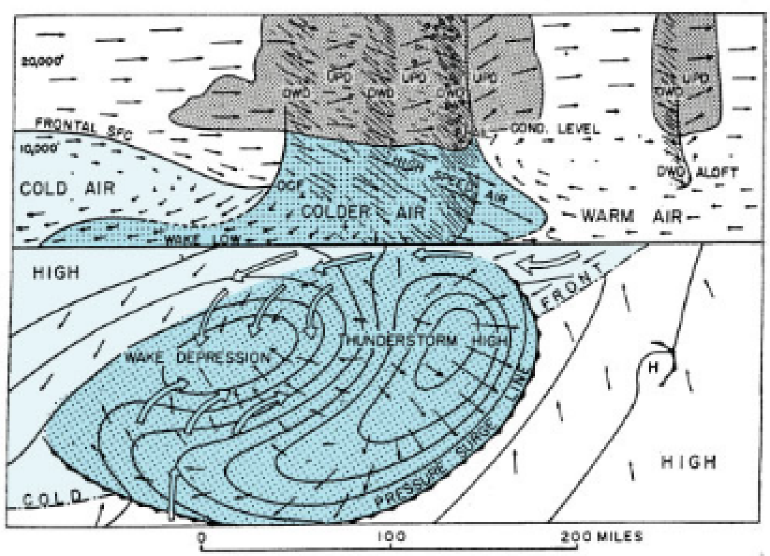

Figure 5.24 Fujita's early model of squall-line circulation, showing high- and low-pressure regions at the surface. (Adapted from Fujita [1955].)

Density current outflow ideas

To first order, outflow boundaries behave like density currents, or gravity currents.

Basic idea is that a gravity wave forms where there is a discontinuity in density.

Differences with synoptic-scale fronts

- Meso-γ scale (order 1 km), so Coriolis doesn't apply
- The density discontinuity can be considered a material surface that is an "impenetrable" interface, for all intents and purposes.

But the outflow boundary itself has very fine scale structures going to the microscale (less than km) - not a "wall"!

- "Lobes and clefts" develop at interface as a result of local dynamic instabilities.
- Local convective overturning, retardation of outflow speed by drag.

Figure 5.25 A density current in a laboratory tank. (Photograph courtesy of Jerome Neufeld and the Experimental Nonlinear Physics Group at the University of Toronto.)

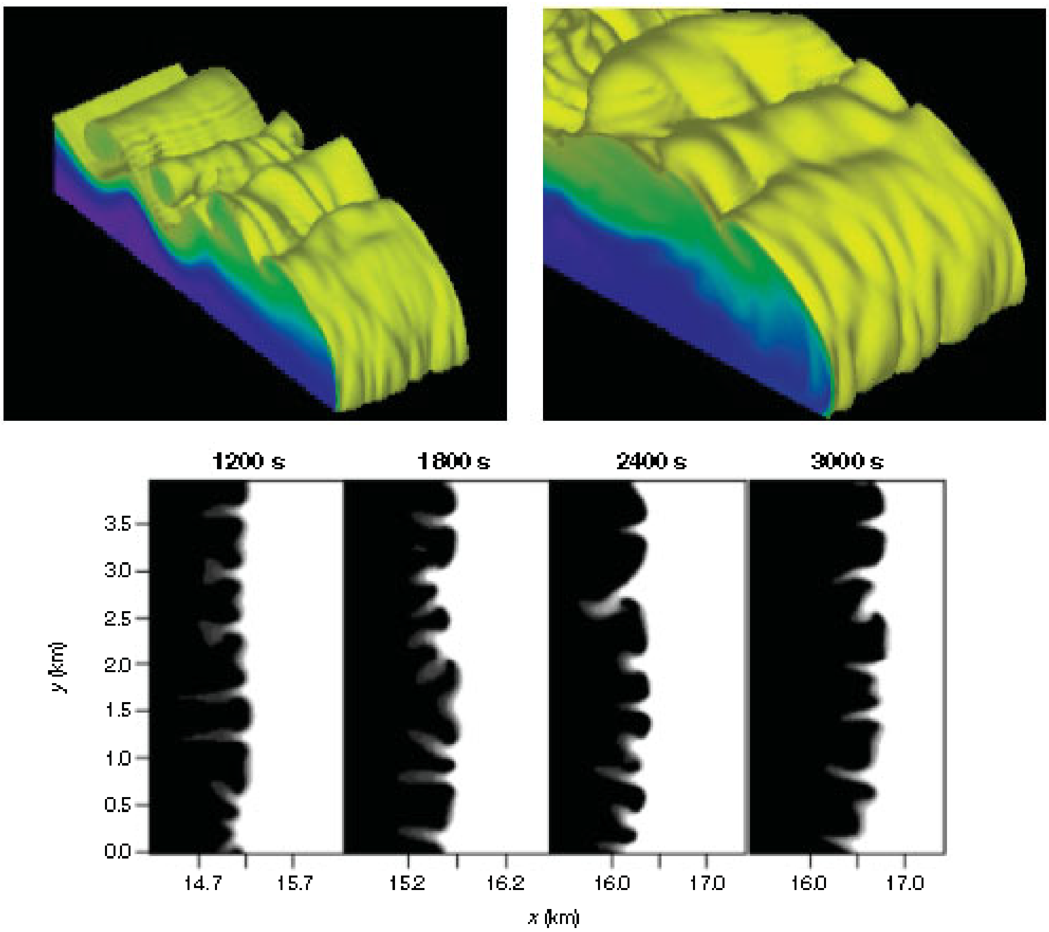

Figure 5.27 Numerical simulation of a density current presenting structures resulting from lobe and cleft instability (top, isosurfaces of potential temperature colder than the ambient potential temperature; bottom, top view of the simulated density current at four select times). Lobe and cleft structures are also evident in the density current shown in Figure 5.25. (Adapted from Lee and Finley [2002].)

Estimating speed of gust front

To first order the speed of gust front is determined by shallow water model theory. This describes gravity wave behavior at the interface of two different fluids with distinct densities

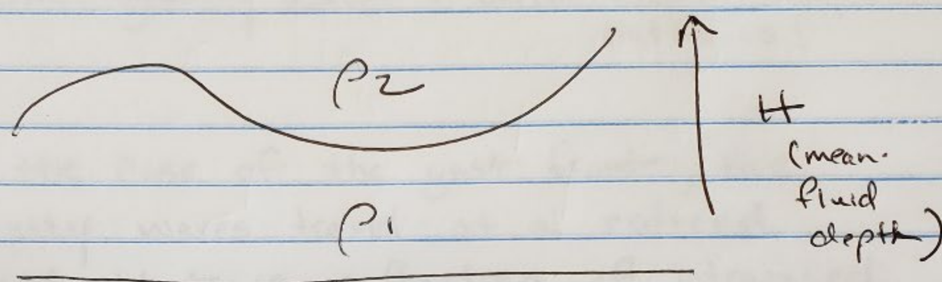

1) Pure shallow water gravity waves

If density discontinuity at the interface is relatively large than $\rho_1 >> \rho_2$

Example: liquid-air interface. In that case, gravity wave speed (c) is

$$\boxed{c = \sqrt{gH}}$$

→ Phase speed of shallow water gravity wave

g = gravitational constant ($9.8\,m/s^2$)

The classic geophysical example of shallow water gravity waves is tsunami waves traveling in ocean. If H is on the order of a few km get waves that travel about the speed of a jet airplane, and can cross an entire ocean on order of 8-12h!

2) Internal gravity wave → better model for outflows!

In the case of the gust front, the gravity waves travel at a reduced speed that is a function of integrated buoyancy through the layer.

$$\int_0^H B\,dz \sim \frac{\rho_2 - \rho_1}{\rho_1} \rightarrow \text{Buoyancy}$$

ρ_2 = density of air within outflow
ρ_1 = density of ambient air.

Get a "reduced" gravity (g')

$$g' = \frac{\rho_2 - \rho_1}{\rho_1} g$$

Speed of outflow is then

$$\boxed{c = K\sqrt{g'H} = K\sqrt{gH\left(\frac{\rho_2-\rho_1}{\rho_1}\right)}}$$

"K" depends on:

- mixing
- surface friction

Theoretical value of "K" = $\sqrt{2}$ (see derivation in text), but estimated to range between 0.7 - 1.3. (near unity)

Our first steps toward Rotunno, Klemp, Wilhelmson (RKW) Theory…

Mesovortices typically develop within mature-to-decaying MCSs. However, so far we have not examined the factors that determine the longevity of MCSs or squall lines. This issue has been studied by Rotunno et al. (1988) [hereafter referred to as RKW], among others. They consider the dynamics of squall lines in terms of the generation of vorticity η about a horizontal axis perpendicular to the squall line by horizontal buoyancy gradients. Referring to the vorticity fields illustrated in Fig. 20, with the x-direction to the right, the vorticity equation is

$$\frac{d\eta}{dt} = -\frac{\partial B}{\partial x} , \tag{7.14}$$

where

$$\eta \equiv \frac{\partial u}{\partial z} - \frac{\partial w}{\partial x} ,$$

Vorticity from wind components in x-z plane

and B = total buoyancy $= g\theta_v'/\bar{\theta}_v$. Using mass continuity,

$$\frac{\partial u}{\partial x} + \frac{\partial w}{\partial z} = 0 ,$$

(7.14) becomes

$$\frac{\partial \eta}{\partial t} = -\frac{\partial}{\partial x}u\eta - \frac{\partial}{\partial z}w\eta - \frac{\partial B}{\partial x} . \tag{7.15}$$

Expand total derivative

Consider the cold pool illustrated below:

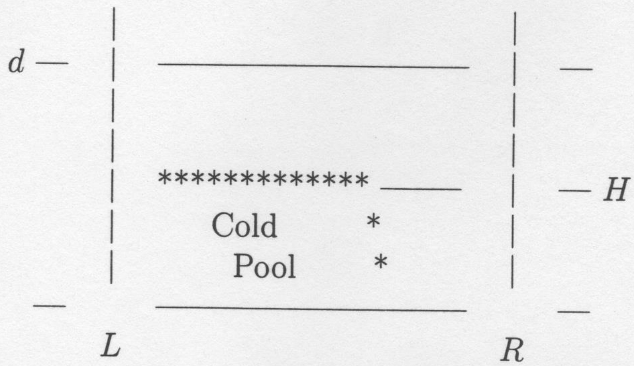

We fix ourselves in a frame of reference moving with the edge of the cold air and integrate (7.15) from a point to the left, $x = L$, to a point to the right, $x = R$, of the cold-air edge, and from the ground to some level, $z = d$, and obtain

$$\underbrace{\frac{\partial}{\partial t}\int_L^R \int_0^d \eta \, dz \, dx}_{\text{tendency}} = \underbrace{\int_0^d (u\eta)_L dz}_{\text{flux at left}} - \underbrace{\int_0^d (u\eta)_R \, dz}_{\text{flux at right}}$$
$$- \underbrace{\int_L^R (w\eta)_d \, dx}_{\text{flux at top}} + \underbrace{\int_0^d (B_L - B_R) dz}_{\text{net generation}} \ . \qquad (7.16)$$

Vorticity tendency =

Net advection of vorticity from sides + difference in buoyancy

Simplifying assumptions

Vertical velocity zero at top

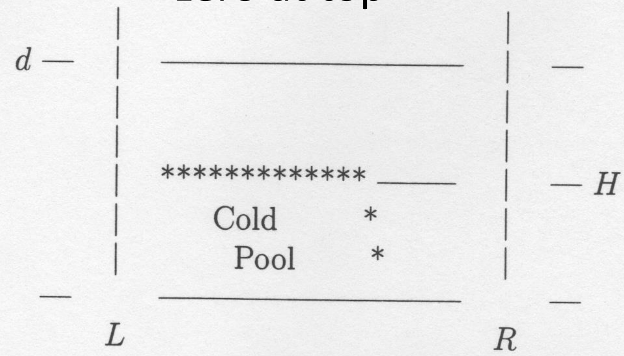

Zonal wind zero on lower left

No shear on right side (u=0)

Since we are looking for a steady balance, we set the tendency term to zero. Also, in the circumstances investigated by RKW, there is negligible buoyancy of the air approaching the cold pool, so $B_R = 0$. Finally, note that $\eta \approx \partial u/\partial z$ away from the edge of the cold air. Under these conditions, (7.16) becomes

$$0 = \left(\frac{u_{L,d}^2}{2} - \frac{u_{L,0}^2}{2}\right) - \left(\frac{u_{R,d}^2}{2} - \frac{u_{R,0}^2}{2}\right) - \int_L^R (w\eta)_d \, dx + \int_0^d B_L dz \; . \tag{7.17}$$

Consider the situation where the cold air is stagnant (relative to the cold-air edge), so $u_{L,0} = 0$, and restricted to a height, $z = H$, where $H < d$. Thus,

$$0 = \frac{u_{L,d}^2}{2} - \left(\frac{u_{R,d}^2}{2} - \frac{u_{R,0}^2}{2}\right) - \int_L^R (w\eta)_d \, dx + \int_0^H B_L \, dz \; . \tag{7.18}$$

Consider first the case where there is no shear at $x = R$ and a rigid plate at $z = d$. Under these conditions the second and third terms on the right-hand-side of (7.18) vanish and we obtain

$$\begin{aligned} u_{L,d}^2 &= 2\int_0^H (-B_L) dz \equiv c^2 \\ &= 2g'H \end{aligned}$$

where $-B_L = -g\Delta\theta/\theta_0 \equiv g'$ and the temperature deficit in the cold pool $\Delta\theta$ has been assumed constant. This reduces to the famous von Kármán formula for speed of gravity current as $d \to \infty$ since $u_{L,\infty} \to u_R$.

Result: zonal wind at the upper boundary travels at the speed of a gravity current due to presence of the cold pool